

Untwisting of the DNA helix stimulates the endonuclease activity of *Bacillus subtilis* Nth at AP sites

Christopher Collier¹, Cristina Machón¹, Geoff S. Briggs¹, Wiep Klaas Smits² and Panos Soultanas^{1,*}

¹Centre for Biomolecular Sciences, School of Chemistry, University of Nottingham, University Park, Nottingham NG7 2RD, UK and ²Department of Medical Microbiology, Leiden University Medical Center, Albinusdreef 2, PO Box 9600, 2300RC, Leiden, The Netherlands

Received June 28, 2011; Revised September 6, 2011; Accepted September 7, 2011

ABSTRACT

Bacterial nucleoid associated proteins play a variety of roles in genome maintenance and dynamics. Their involvement in genome packaging, DNA replication and transcription are well documented but it is still unclear whether they play any specific roles in genome repair. We discovered that untwisting of the DNA double helix by bacterial non-specific DNA binding proteins stimulates the activity of a repair endonuclease of the Nth/MutY family involved in abasic site removal during base excision repair. The essential *Bacillus subtilis* primosomal gene *dnaD*, coding for a protein with DNA-untwisting activity, is in the same operon with *nth* and the promoter activity of this operon is transiently stimulated by H₂O₂. Consequently, *dnaD* mRNA levels persist high upon treatment with H₂O₂ compared to the reduced mRNA levels of the other essential primosomal genes *dnaB* and *dnaI*, suggesting that DnaD may play an important role in DNA repair in addition to its essential role in replication initiation. Homologous Nth repair endonucleases are found in nearly all organisms, including humans. Our data have wider implications for DNA repair as they suggest that genome associated proteins that alter the superhelicity of the DNA indirectly facilitate base excision repair mediated by repair endonucleases of the Nth/MutY family.

INTRODUCTION

Molecular crowding, supercoiling and genome-associated architectural proteins, collectively known as nucleoid associated proteins (NAPs), fold the bacterial chromosome

into a compact structure by bridging, bending or wrapping the DNA (1–5). NAPs are implicated in initiation of DNA replication (6), chromosome segregation (7) and transcription (8–13), but their potential roles in DNA repair have not been explored in detail. When DNA repair pathways are hindered, the bacterial nucleoids are organized into morphologies that promote DNA repair and protection (14). The roles of various NAPs in these responses and their links to DNA repair are not fully understood. They may, directly through protein–protein interactions or indirectly by affecting the superhelical properties of the DNA substrates, modulate the functions of repair enzymes. Alternatively, by locally increasing or decreasing local compaction they may affect access to damaged sites by repair enzymes.

In *Bacillus subtilis*, and other low G+C content gram positive bacteria, the essential primosomal proteins DnaD and DnaB are involved in loading the replicative helicase DnaC at the replication origin, *oriC* (15–17), and at sites of replication fork collapse across the genome (17,18). The two proteins are structurally related (19,20) and multi-functional, exhibiting significant DNA remodelling activities consistent with NAPs (21–24). In *B. subtilis*, DnaD comprises two domains DDBH1–DDBH2 (DnaD DnaB Homologies 1 and 2) whereas DnaB has a central redundant DDBH2 domain spanned by a DDBH1 domain at the N-terminus and a DDBH2 domain at the C-terminus (19). The DDBH1 domains mediate DNA-independent oligomerization while the DDBH2 domains mediate DNA-binding and a second DNA-dependent oligomerization activity (19,20,23).

DDBH1 contains a WH (Winged Helix) motif with a helix-strand-helix inserted at its N-terminus and an extra helix at its C-terminus (19,25). DDBH2 is a helical bundle with a highly conserved YxxxIxxxW sequence that contributes to DNA binding together with a solvent exposed somewhat unstable helix and a mobile C-terminal

*To whom correspondence should be addressed. Tel: +44 115 9513525; Fax: +44 115 8468002; Email: panos.soultanas@nottingham.ac.uk

unstructured region (19). Proteolysis of this unstructured C-terminal region *in vivo* appears to regulate its oligomerization and localization at the *oriC* (20). *B. subtilis* DnaD forms large scaffolds that ‘open up’ supercoiled DNA by increasing negative twist (untwisting the double helix) and at the same time eliminating writhe, while DnaB laterally compacts DNA without affecting DNA supercoiling (22,24,26). The DDBH1 and DDBH2 domains must be physically linked for DnaD to exhibit its effective DNA remodeling activity (23). Binding of the DDBH2 to DNA can cause some untwisting of the DNA duplex, albeit not as effective as native DnaD (24,26).

The *dnaB* gene is juxtaposed with the helicase loader *dnaI* gene in the same operon, consistent with its proposed essential function as co-loader of the replicative helicase, DnaC (27–29). The *dnaD* gene is juxtaposed with the *nth* gene coding for an endonuclease III of the Nth/MutY family of DNA repair glycosylases (30). They belong to a wider HhH (Helix hairpin Helix) superfamily of glycosylases and are highly conserved across bacteria, archaea and eukaryotes (31). Nth is involved in BER (Base Excision Repair). It targets abasic AP (Apyrimidinic) lesions and cleaves the C-O-P bond 3' to the AP site by a β -elimination reaction, leaving a nick with a 3'-terminal unsaturated sugar and a terminal 5' phosphate (32,33). The nick is then processed by repair enzymes to eventually eliminate the lesion. It is well established that functionally linked bacterial genes are often clustered together in the same operon for coordinated, efficient and rapid responses to environmental and nutritional stimuli. The juxtaposition of the *dnaD* and *nth* genes in the same operon in *B. subtilis* raises the possibility of functional cooperation.

Here, we investigated the effect of DnaD on Nth activity and found that DnaD stimulates the endonuclease activity of Nth on AP-containing supercoiled DNA substrates *in vitro*. We propose that this stimulatory effect is mediated indirectly via the duplex untwisting activity of DnaD. In support of this, we established that *B. subtilis* YonN, a homolog of the bacterial NAP HBSu coded for by the SP β prophage *yonN* gene, and HBSu also untwist the DNA duplex and similarly stimulate the Nth activity. By comparison, DnaB, which does not alter DNA supercoiling, does not affect the Nth activity. We conclude that untwisting of the DNA duplex enhances the endonuclease activity of Nth at AP sites. We show that deletion of the *nth* gene results in a strain sensitive to H₂O₂ exposure, suggesting that Nth plays a prominent role in the oxidative damage response. Furthermore, we show that the *dnaD-nth* operon is constitutively active and transiently stimulated by H₂O₂. Furthermore, the *dnaD* mRNA levels persist at relatively high levels compared to the reduced mRNA levels of the other two primosomal proteins *dnaB* and *dnaI*. These data suggest that DnaD may play an important role in DNA repair in addition to its essential role in the initiation of DNA replication. We conclude that NAP proteins with DNA untwisting activities facilitate Nth-mediated BER.

EXPERIMENTAL PROCEDURES

Bacterial strains and plasmids

All bacterial strains and plasmids used in this work are listed in Supplementary Figure S1.

Protein purifications Nth

The *nth* gene was cloned by PCR from *B. subtilis* strain 168 genomic DNA into the NcoI and XhoI sites of pET28a (Novagen) to create the pET28a-*nth* plasmid. This was transformed into BL21 (DE3) *Escherichia coli* and 10 ml overnight LB (Luria Bertani) cultures were obtained from single colonies. An overnight culture was used to inoculate a 1 l of LB containing kanamycin (30 $\mu\text{g ml}^{-1}$) and incubated at 12°C with vigorous shaking. At an OD₅₉₅ = 0.6, 1 mM IPTG was added to induce expression of the Nth protein (Native MW 24 853 Da) and the culture was left to grow for ~86 h. Cells were harvested at 5000g for 15 min, and suspended in 40 ml of binding buffer (50 mM phosphate buffer, pH 8.0, 5 mM imidazole and 250 mM NaCl), sonicated in the presence of a protease inhibitor cocktail (Sigma p8849), and the suspension was clarified by centrifugation for 30 min at 40 000g. The supernatant was filtered before loading onto a 5 ml HisTrap HP column (GE Healthcare) equilibrated in binding buffer. Protein was eluted over 150 ml with a 0–100% gradient of elution buffer (50 mM phosphate buffer, pH 8.0, 1 mM DTT and 500 mM imidazole). Nth-containing fractions were pooled and loaded onto a 5 ml HiTrap heparin column (GE Healthcare), equilibrated in TED₀ (50 mM Tris, pH 7.5, 1 mM EDTA, 1 mM DTT), keeping the conductivity at <8 ms during loading. Protein was eluted over 120 ml with a 2–40% gradient of elution buffer TED_{2M} (50 mM Tris, pH 7.5, 1 mM EDTA, 1 mM DTT, 2 M NaCl). Nth-containing fractions were pooled and the volume reduced using 10 kDa cut-off concentrator spin columns (Amicon) to 5 ml which was then loaded onto a HiLoadTM SuperdexTM S75 gel filtration column (GE Healthcare), equilibrated in TED₂₅₀ (50 mM Tris, pH 7.5, 1 mM EDTA, 1 mM DTT, 250 mM NaCl). Nth-containing fractions were pooled, made up to 10% v/v glycerol, the concentration determined spectrophotometrically at 280 nm using the extinction coefficient 0.17 M⁻¹cm⁻¹ and aliquots were flash frozen in liquid nitrogen for storage in –80°C.

Nth was highly pure with no other bands visible on SDS-PAGE gels even when grossly overloaded samples of 400 μM were analysed (Supplementary Figure S2). The *E. coli* endonuclease III homolog of Nth contains an [4Fe-4S]⁺ cluster that plays primarily a structural role (34). Predictably, *B. subtilis* Nth exhibited a deep brown colour characteristic of [4Fe-4S]⁺ cluster containing proteins. Solvent-exposed [4Fe-4S]⁺ clusters in proteins are sensitive to oxidation resulting to univalent demetallation to [3Fe-4S]⁺ which can lead to protein instability and functional inactivation [(35) and references therein]. To establish whether the *B. subtilis* Nth [4Fe-4S]⁺ cluster is prone to air oxidation, Nth was buffer exchanged into TE₃₀₀ buffer (50 mM Tris, pH 7.5, 1 mM EDTA,

300 mM NaCl) and incubated at room temperature for up to 5 h. UV-visible light absorption spectra in the 235–748 nm range were obtained from samples at 0, 1.5, 2.5 and 5 h (Supplementary Figure S3). The characteristic absorption maximum at 420 nm was observed. All spectra were identical with no discernible difference in absorption at 420 nm. Furthermore, the colour of the Nth solution did not fade over time. Collectively these data indicate that the [4Fe-4S]⁺ cluster is not prone to air oxidation. Therefore, under our experimental conditions the Nth protein was considered to be stable.

YonN

The *yonN* gene was cloned by PCR from *B. subtilis* strain 168 genomic DNA into the NdeI and HindIII sites of pET28b to create the pET28b-*yonN* plasmid for expression of a C-terminal hexahistidine tagged YonN. This was transformed into BL21 (DE3) *E. coli* and 10 ml overnight LB cultures were obtained from single colonies. An overnight culture was used to inoculate 1 Lt of LB containing kanamycin (30 µg ml⁻¹) and incubated at 37°C with vigorous shaking. At OD₅₉₅ = 0.6 YonN (Native MW 9714 Da) expression was induced with 1 mM IPTG for 3 h. Cells were harvested at 5000g for 15 min and suspended in 40 ml binding buffer (50 mM phosphate buffer, pH 8.0, 1 mM DTT, 5 mM imidazole and 500 mM NaCl). Around 1 mM of Phenylmethyl Sulfonyl Fluoride (PMSF) was added prior to sonication. The suspension was clarified by centrifugation at 40 000g for 30 min and the supernatant loaded onto a 5 ml HisTrap HP column equilibrated in binding buffer. YonN was eluted over 150 ml from 0–100% of elution buffer (50 mM phosphate buffer, pH 8.0, 1 mM DTT, 500 mM imidazole and 500 mM NaCl). The appropriate fractions were pooled and the protein precipitated with ammonium sulphate (29 g per 100 ml⁻¹). The protein was centrifuged at 40 000g for 30 min and the pellet suspended in 8 ml TED₀. The sample was filtered and injected onto a HiLoadTM SuperdexTM S75 26/60 gel filtration column equilibrated in TED₀. YonN-containing fractions were pooled and made up to 10% v/v glycerol. YonN does not contain tryptophans, tyrosines or cysteines and therefore does not absorb light at 280 nm. It does not give a proportionally increasing signal in a Bradford assay and hence its concentration was obtained by comparison of serial dilutions against a known control (Lysozyme) in an SDS-PAGE gel. Aliquots were flash frozen in liquid nitrogen for storage in -80°C.

HBsu

The *hbs* gene was amplified from the plasmid pHM9 (gift from Alan Grossman, MIT) using the primers 5'-AGG AGA CCA CAT ATG AAC AAA ACA-3' and 5'-TGC GGC CGC AAG CTT TTA ATG ATG-3' and cloned into the NdeI and HindIII sites of pET22b (Novagen) creating the pET22b-HBsu plasmid coding for a C-terminal His-tag HBsu. This was transformed into BL21 (DE3) pLysS *E. coli* and 10 ml overnight LB cultures were obtained from single colonies. An overnight culture was used to inoculate 11 of 2×YT containing

chloramphenicol (30 µg ml⁻¹) and ampicillin (100 µg ml⁻¹) and incubated at 37°C with vigorous shaking. At OD₅₉₅ = 0.6 HBsu (Native MW 9746 Da) the temperature was lowered to 30°C and protein expression induced by IPTG (0.2 mM) for 4 h. Cells were harvested at 5000g for 15 min, suspended in 40 ml buffer B (50 mM Tris-HCl, pH 7.5, 0.5 M NaCl) and lysed by sonication. The suspension was clarified by centrifugation at 40 000g for 30 min and the supernatant loaded onto a 5 ml HisTrap HP column equilibrated in buffer B supplemented with 0.03 M imidazole. HBsu was eluted with buffer B supplemented with 0.25 M imidazole. The appropriate fractions were pooled and loaded onto a SuperdexTM S75 26/60 gel filtration column equilibrated in buffer A (50 mM Tris-HCl, pH 7.5, 1 mM EDTA, 1 mM DTT) supplemented with 100 mM NaCl. HBsu containing fractions were pooled and loaded to a 5 ml heparin HiTrap HP column (GE Healthcare) equilibrated in buffer A. HBsu was eluted with buffer A supplemented with 0.8 M NaCl. Like YonN, HBsu does not contain tryptophans, tyrosines or cysteines and does not give a proportionally increasing signal in a Bradford assay. Its concentration was determined in the same manner as that of YonN.

DnaD and DnaB

DnaD (Native MW 27 490 Da) and DnaB (Native MW 54 722 Da) were purified and quantified as described previously (21,22). The proteins were stored in -80°C in TED₃₀₀ (50 mM Tris, pH 7.5, 1 mM EDTA, 1 mM DTT, 300 mM NaCl) supplemented with 10% v/v glycerol for DnaD, and TED₁₀₀ (50 mM Tris, pH 7.5, 1 mM EDTA, 1 mM DTT, 100 mM NaCl) supplemented with 10% v/v glycerol for DnaB.

Generation of abasic sites

Abasic sites were generated on supercoiled pBSK plasmid as described elsewhere (36). Briefly, pBSK (100 nM) was incubated for 8 min with AP citrate buffer (0.1 mM NaCl, 0.01 mM citrate, pH 5.0) at 70°C. Under these conditions on average two AP sites per plasmid molecule are generated (37). Gel solubilisation buffer (Sigma GenElute Gel Extraction kit) was added along with isopropanol and the extraction procedure was followed according to the manufacturer's instructions. The AP-containing pBSK was finally eluted in 10 mM Tris-HCl, pH 9.0. The presence of AP sites was verified by fluorescence using the FARP (Fluorescent Aldehyde Reactive Probe), Alexa Fluor[®] 488 C₅-aminoxyacetamide bis(triethylammonium) salt (Alexa Fluor[®] 488 hydroxylamine) (Invitrogen), as described elsewhere (38). Briefly, the fluorophore was suspended in 1 ml DMSO (Dimethyl Sulphoxide) for storage and freshly diluted as appropriate for experimental use. AP-containing and control pBSK of varying concentrations were incubated separately with 100-fold excess of the fluorophore and incubated at room temperature for 4 h in the dark under gentle rotation. The plasmid DNA was then isolated by two successive ethanol precipitations, which removed excess unbound fluorophore, and finally suspended in 10 mM HEPES and 1 mM EDTA, pH 7.4. To verify the creation of AP lesions, equimolar

concentrations of AP-containing and control pBSK were run on a Perkin Elmer LS 55 luminescence spectrophotometer with an emission slit width of 5 nm, excitation slit width of 2.5 nm, excitation wavelength of 488 nm and emission detection between 500 and 600 nm.

Nth nicking assays

Nth nicking assays were carried out with AP-containing and control supercoiled pBSK (7.14 nM) incubated at 37°C with Nth (0.05–5 nM) for 1–15 min in 20 mM Tris–HCl, pH 7.0, 2 mM EDTA, 1 mM DTT and 250 mM NaCl. Proteinase K was added for 30 min and pBSK was resolved through 1% w/v agarose gels in TAE (40 mM Tris-base, pH 8.0, 1 mM EDTA and 20 mM acetic acid). Under these conditions Nth-mediated nicking was detected rapidly (<1 min), by the conversion of supercoiled to open circular pBSK, and the percentage nicking did not increase significantly after that time point (data not shown). The assay essentially detects only the first nick at an AP site as further nicks at additional sites on the same plasmid molecule will not be detected. The DNA was stained with ethidium bromide and quantification was carried out using a G:BOX gel imaging system with its associated Gene Tools software (SynGene). All experiments were carried out in triplicate.

Determining the effects of NAPs on Nth nicking activity

AP-containing pBSK (7.14 nM) was incubated with DnaD (10.0 μM), YonN (9.7 μM) or DnaB (53 μM) for 10 min at 37°C, followed by the addition of 0.5–1 nM Nth for 1–15 min. The reactions were terminated by addition of proteinase K for 30 min and pBSK was resolved through 1% w/v agarose gels in TAE. Control reactions were set up with only Nth and the appropriate buffers added instead of the other proteins. Further experiments with control pBSK plasmid (without AP sites) were carried out in a similar manner. All experiments were carried out in triplicate.

Topoisomerase I assays

Assays to establish the untwisting activities of YonN and HBSu were carried out as described before for DnaD (26).

Creation of the *B. subtilis* *Anth*(cat) strain

The *B. subtilis* *Anth*(cat) strain was created by double crossover integration of the chloramphenicol acetyl transferase (*cat*) gene at the *nth* locus, and selecting for chloramphenicol resistance. The upstream and downstream flanking regions (~1000 bp on either side) of the *nth* gene were amplified from genomic DNA using the PSnthFO (5'-ATCGCGTCTTAAAGAACATGGACTG GATTCTG-3') and PSnth/catRE (5'-**TACCGCACAGAT CCGTAAGGAGGATTGTACCTTTTCACTTTATTG TTCAAGCC**-3'), the bold underlined sequence is complementary to the beginning of the *cat* gene) for the upstream region, and the PSnthRE (5'-AACAGCCGTCAGTGAT GATGGCAAAGTACAG-3') and PSnth/catFO (5'-**TA ATATGAGATAATGCCGACTGTACTTTGACGCAAG CAAAAGAAGTGTGGCTTCCTTAT**-3'), the bold

underlined sequence is complementary to the end of the *cat* gene) for the downstream region. The products from these amplifications were used as primers in a PCR with the pGEMcat plasmid (39) as substrate to splice by overlap the *nth* upstream and downstream regions at the front and back of the *cat* gene, respectively. The product of this PCR was used as substrate with the PSnthFO and PSnthRE primers to amplify it further by PCR, and the final product was used to transform competent wild type *B. subtilis* cells. Selection of positive transformants was carried out on chloramphenicol plates. Single colonies were used to inoculate LB/Chloramphenicol cultures (5 ml) which were grown to late logarithmic phase. Cells were harvested and genomic DNA prepared from these cells was used to back cross with wild type *B. subtilis* to select the final Δ *nth*(cat) strain by chloramphenicol resistance. Deletion of *nth* was finally confirmed by PCR using the PSnthFO–PSnthRE and OMM (5'-CTCTATTCAGG AATTGTCAGATAGG-3', annealing near the end of the *cat* gene)–PSnthRE primer pairs to amplify the entire *cat*-containing insertion and a fragment containing part of the *cat* gene and the downstream *nth* region (data not shown). Control reactions with genomic DNA from the wild type *B. subtilis* strain 168 were used for comparison (data not shown).

H₂O₂ sensitivity experiments

The wt *B. subtilis* 168 and *Anth*(cat) strains were grown from fresh single colonies in LB at 30°C to an OD₆₀₀ of 0.12 and 0.14, respectively. Samples (1 ml) were removed and H₂O₂ was added (22, 45, 60, 90, 120, 150 and 180 mM). Distilled water instead of H₂O₂ was added to the control samples. All samples were incubated for 30 min at 30°C with vigorous shaking, before serial dilutions were spotted on LA plates and left to grow at 30°C overnight.

β-galactosidase reporter assays

To generate the *lacZ* reporter construct for the *dnaD*-*nth* promoter (P_{dnaD}), a 600 bp DNA fragment immediately upstream from the ATG start codon of *dnaD* was isolated by PCR using genomic DNA from *B. subtilis* strain 168 and the primers proFO (5'-AGACAC**GAAATTC**GTCAA ACTTGAGCAAATC-3', the bold underlined sequence is the EcoRI site) and proRE (5'-TTTT**CAGGATCCT**CGT CACACCTTACTGT-3', the bold underlined sequence is the BamHI site), and then directionally cloned in the EcoRI and BamHI sites in front of the promoterless *lacZ*-*spoVG* fusion of the pDG268 plasmid (40) with a *cat* marker. The entire cassette with the *cat*-P_{dnaD}-*spoVG*-*lacZ* was inserted in the *amyE* locus by double cross over integration and the sequence was confirmed by sequencing. Positive transformants were isolated by chloramphenicol selection and genomic DNA from these was transformed back to the wt *B. subtilis* strain 168 to obtain the final P_{dnaD}-*lacZ* strain by chloramphenicol selection. The correct insertion at the *amyE* locus was confirmed by PCR (data not shown). As an additional control, the promoterless *cat*-*spoVG*-*lacZ* fragment was

also integrated at the *amyE* locus in exactly the same manner to obtain the final *B. subtilis lacZ* control strain.

β -Galactosidase reporter assays were carried out as described elsewhere (41). Briefly, a 15 ml LB culture was grown at 30°C overnight from a single colony. At an $OD_{600} = 0.6$ H_2O_2 (0.1 mM) was added, with the equivalent volumes of dH_2O added to the respective control cultures. Aliquots (0.5 ml) were taken at 2, 5, 7, 10, 15 and 20 min. The cells were collected by centrifugation at 13 000 r.p.m. for 10 min, suspended in 1 ml of 100 mM sodium phosphate, pH 7.0, 10 mM KCl, 1 mM Mg_2SO_4 and 4 mM β -mercaptoethanol, and lysed at 30°C for 2 min by adding 50 μ l of chloroform and 25 μ l of 0.1 % v/v SDS. The reaction was initiated by the addition of 200 μ l of ONPG (*ortho*-nitrophenyl- β -galactosidase) (4 mg μ l⁻¹) in each sample and vortexing. After 30 min at 30°C the reaction was stopped with 0.5 ml 1 M Na_2CO_3 . Absorbance values at 410, 550 and 650 nm were recorded and the β -galactosidase activity was determined using the equation

$$\text{Miller units} = \frac{[\text{OD}_{420} - (1.75 \times \text{OD}_{550})] \times 1.775}{[\text{OD}_{650} \times T \times V \times 0.0045]}$$

where 1.775 ml is the total reaction volume, T = time of the reaction in minutes, V = volume (ml) of cells added, $0.045 \mu\text{M}^{-1}\text{cm}^{-1}$ is the extinction coefficient of *o*-nitrophenol at OD_{420} .

RT-PCR

Bacillus subtilis strain 168 was cultured in LB. An overnight culture was diluted into fresh LB and incubated at 30°C. At an $OD_{600} = 0.3$ – 0.4 the culture was divided in two and 80 mM H_2O_2 was added to one of the media with the equivalent volume of sterile dH_2O added to the control. After 30 min incubation, 4 ml samples were collected for RNA extraction, quantification and quality control check as described before (20).

Primers for the RT-PCR were designed with Primer Express 3.0 software (PE Applied Biosystems) for *dnaB*, *dnaD*, *dnaI* genes and the endogenous control *rrnO-16S* ribosomal RNA (42): *dnaB*-forward (5'-CTGCCCGATT TGGTGGAA-3'), *dnaB*-reverse (5'-CCGGTTGTTCCGCC TTCAC-3'), *dnaD*-forward (5'-CCGTTATCGCCTTTGG AGTGT-3'), *dnaD*-reverse (5'-TTGTGCGTCATGCTGA TCCT-3'), *dnaI*-forward (5'-CGGAAGATGAAACTG CAACA-3'), *dnaI*-reverse (5'-AGACCTCCCATGAC AACAAAGCT-3'), 16S-forward (5'-AGCGATGTGCGT AGTCAGTCAA-3') and 16S-reverse (5'-TGCGGCGA CACCTGTGT-3'). RT-PCR reactions were carried out as described before (20). Relative quantification was used, as described before (20), to determine change in expression of *dnaB*, *dnaD* and *dnaI* genes compared to *r16S* (ΔC_T value), followed by comparison of the change in expression of the three genes incubated with H_2O_2 compared to the control sample ($\Delta\Delta C_T$ value). All results were expressed as the mean of triplicate assays \pm standard deviation. Statistical analysis was carried out with the StatsDirect 2.5.8 software package, applying a parametric paired *t*-test to test for the mean difference in

ΔC_T value for each gene in the presence versus absence of H_2O_2 in the three experiments (data not shown).

RESULTS

Creation of abasic sites in supercoiled DNA

Treatment of plasmid DNA for 8 min with a citrate buffer at 70°C has been shown before to create AP sites in a controlled manner (on average two AP sites per plasmid molecule) [(36,37) and references there in]. However, this method does not control the uniform distribution of AP sites across all plasmid molecules. Inevitably, the population of AP-containing plasmid molecules will consist of a mixture of molecules some containing 0, 1, 2 or even more AP sites giving a total average of two AP sites per plasmid. Following this procedure we treated pBSK with citrate buffer for different times over a period of 30 min to generate AP sites and, at the same time, to establish the best experimental conditions for preserving the superhelicity of the plasmid and minimize acid-induced nicking (Supplementary Figure S4A). The optimal experimental conditions were established to be identical to those published before [(36,37) and references there in], 8 min treatment at 70°C. The presence of AP lesions was verified by fluorescence using a FARP. The AP-containing pBSK exhibited greater fluorescence than the control pBSK, characteristic of FARP binding to AP sites (Supplementary Figure S4B). Using such AP-containing supercoiled pBSK plasmids we were able to assay the activity of Nth. The enzyme acted specifically on the AP-containing pBSK to nick it hence converting the supercoiled pBSK to an open circular form that migrated slower through agarose gels (Figure 1). Under the conditions of our assay, Nth did not exhibit any significant nicking activity on control pBSK without AP sites (Figure 1). Our assay reports on Nth-mediated nicking at an AP site by conversion of supercoiled plasmid to open circular but even though the enzyme is 'turning over' additional nicks on the same plasmid molecule are silent and undetected. The presence of a mixed population of plasmid molecules some of which contain no AP sites as explained above is consistent with the failure of Nth to nick 100% of the AP-containing plasmid indicating that a proportion of the plasmid substrate contains no AP sites. The exceptionally high purity and high concentration of purified stock Nth (Supplementary Figure S2) makes it highly unlikely that the observed nicking activity and its stimulation by DnaD are the result of a contaminant protein in our assays. For a contaminant activity to be detected it should be extremely and unusually hyperactive as well as exclusively targeting AP sites and stimulated by DnaD. This is a highly unlikely and improbable scenario. It is, therefore, safe to conclude that the AP-specific nicking observed is the result of Nth activity.

DnaD stimulates the Nth activity

Agarose gel shift assays were used to determine the optimum DnaD concentration at which pBSK (7.14 nM) starts to shift, indicative of extensive binding of DnaD [Supplementary Figure S5A and (22,23,26)]. We have

shown before that multiple DnaD molecules bind to supercoiled plasmid forming a large scaffold that shifts higher up in agarose gels during electrophoresis (20–25). Treatment of the pBSK-DnaD binding mixtures with proteinase K prior to gel electrophoresis digested the DnaD, and the pBSK plasmid reverted to its original supercoiled state (evident from its migration position through the

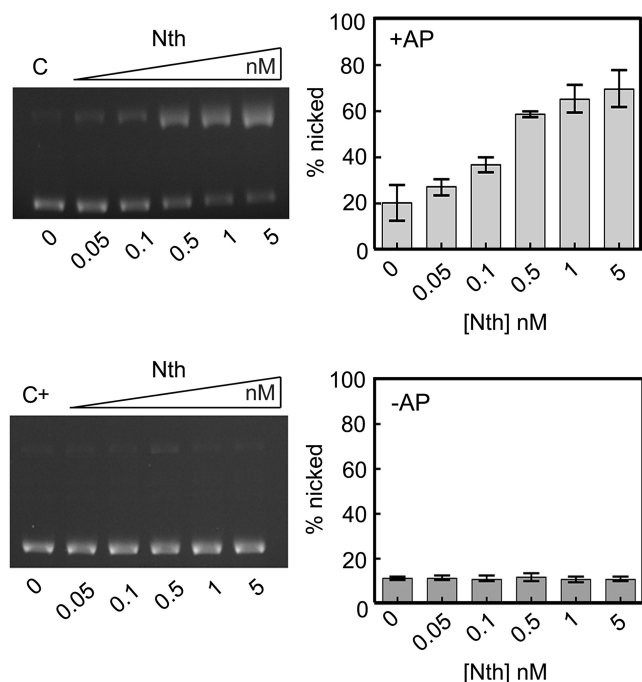


Figure 1. Nth specifically nicks AP-containing pBSK. Typical gels showing plasmid nicking by increasing concentrations of Nth (0.05, 0.1, 0.5, 1 and 5 nM) incubated with AP containing (+AP) and control (–AP) pBSK (7.14 nM) plasmid for 15 min, as indicated. After treatment with proteinase K, samples were resolved through 1% w/v agarose gels. Controls represent +AP (C+) and –AP (C–) pBSK (7.14 nM) incubated for 15 min in the absence of Nth. Quantification of the percentage nicking is shown in bar graphs with error bars indicating standard error (SE) of the mean from triplicate experiments.

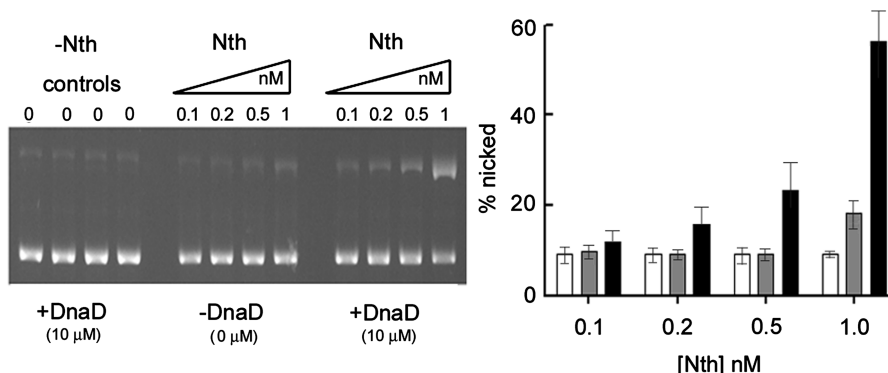


Figure 2. DnaD stimulates the activity of Nth. Nicking assays were carried out with increasing concentrations of Nth (0.1, 0.2, 0.5 and 1.0 nM) for 5 min in the presence or absence of DnaD (10 μM) and 7.14 nM pBSK as indicated. Control reactions were carried out with 7.14 nM pBSK in the presence of DnaD (10 μM) and in the absence of Nth. The amount of nicked pBSK, as a percentage of the total, is indicated by bar graphs (white, grey and black bars show control, Nth and Nth+DnaD reactions, respectively). Quantification of the percentage nicking is shown in bar graphs with error bars indicating SE from triplicate experiments.

agarose gel during electrophoresis) confirming previous reports that DnaD does not nick supercoiled DNA (Supplementary Figure S5A and (22,23,26)]. The optimum concentration under our experimental conditions was established to be 10 μM of DnaD which is compatible with previously published data (22,23,26). This concentration was used to investigate whether DnaD affects the activity of Nth. Using nicking assays we found that binding of DnaD to pBSK stimulates the nicking activity of Nth on AP-containing supercoiled pBSK (Figure 2).

In order to establish whether this stimulatory effect is mediated by a direct protein-protein interaction analytical gel filtration, Isothermal Titration Calorimetry (ITC), Surface Plasmon Resonance (SPR) and glutaraldehyde fixing experiments were carried out with purified DnaD and Nth proteins. Despite our extensive efforts no direct DnaD-Nth interaction was detected with any of these experimental techniques (data not shown). In the absence of evidence for an Nth-DnaD interaction, an alternative explanation for the stimulation of the Nth activity was considered. We hypothesized that DnaD, via its DNA remodelling activity, alters the DNA substrate rendering it more susceptible to the Nth activity. DnaD has been shown to form large scaffolds with DNA and to eliminate writhe of supercoiled plasmids by increasing the negative twist (22,24,26). We further hypothesized that if Nth stimulation is mediated by the untwisting of the DNA duplex, other proteins that also untwist the DNA duplex could have similar effects on the activity of Nth.

YonN and HBSu untwist the DNA helix and stimulate Nth but DnaB does not

YonN is a small protein located in the SPβ prophage of the *B. subtilis* genome (43). It is homologous to HBSu, both proteins being of equal length (92 amino acid residues) and sharing 68.5% identity (Supplementary Figure S6). HBSu is a homodimeric homolog of the *E. coli* heterodimeric HUαβ. HU proteins from *E. coli*, *Thermotoga maritima*, *Borrelia burgdorferi* and *Anabaena* have been widely reported to bind to supercoiled DNA

and increase negative supercoiling (44–47). Consistent with these studies, we established that YonN and HBSu also increase negative supercoiling. Incubation of pBSK with increasing concentrations of YonN or HBSu stimulated the activity of topoisomerase I (Figure 3A). As more negative supercoiling was introduced, by increasing concentrations of YonN or HBSu, topoisomerase I progressively relaxed the additional negative supercoils by introducing positive linking number changes. Subsequent removal of all the proteins by proteinase K treatment left behind supercoiled pBSK with progressively higher positive linking number changes resulting in the appearance of more relaxed plasmid higher up the gel (Figure 3A). Neither YonN nor HBSu possessed any nicking activity since incubation with high concentrations of these proteins with pBSK and their subsequent removal by proteinase K treatment resulted in fully supercoiled plasmid without any detectable nicking [Supplementary Figure S5 and (22,23,26)]. From these data we conclude that both YonN and HBSu bind to supercoiled DNA and untwist the DNA double helix.

We then investigated whether YonN or HBSu can affect the nicking activity of Nth. Agarose gel shift assays were first used to determine the optimum YonN and HBSu concentrations at which pBSK (7.14 nM) starts to shift, indicative of extensive protein binding (Supplementary Figure S5B and C). Treatment with proteinase K digested the YonN or HBSu in the reaction mixtures, and the pBSK plasmid reverted to its original supercoiled state, confirming that YonN and HBSu do not nick supercoiled DNA (Supplementary Figure S5B and C). The optimum concentrations under our experimental conditions were established to be 9.72 and 10 μM for YonN and HBSu, respectively. These concentrations were used to investigate whether YonN and HBSu affect the activity of Nth in assays similar to those carried out for DnaD. We found that binding of YonN or HBSu to pBSK stimulated the nicking activity of Nth on AP-containing supercoiled pBSK (Figure 3B). By comparison, the primosomal protein DnaB, which is involved with DnaD in the initiation of DNA replication in *B. subtilis* and shown previously to form large complexes with supercoiled DNA without altering DNA superhelicity (22,26), formed large complexes with supercoiled pBSK [Supplementary Figure S7C and (22)] and did not stimulate the Nth nicking activity in our assay (Figure 3C). From the combined data we conclude that non-specific DNA binding proteins such as DnaD, YonN and HBSu that increase negative supercoiling stimulate the nicking activity of Nth, whereas non-specific DNA binding proteins such as DnaB that do not affect DNA supercoiling do not affect the activity of Nth.

Deletion of *nth* increases sensitivity to H_2O_2

In order to verify the putative role of Nth in oxidative damage response, the *nth* gene was deleted by a double cross over insertion of a fragment carrying the *cat* gene flanked by 1-bp sequences from the upstream and downstream regions of *nth*. The deletion was verified by PCR (data not shown). In comparative experiments the

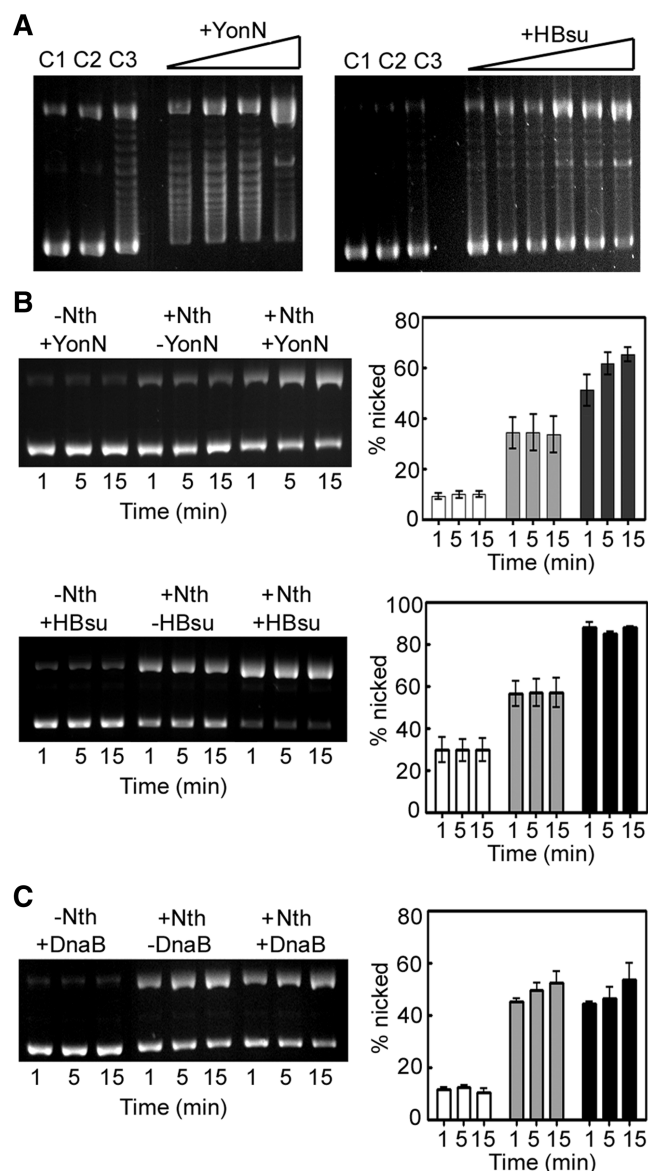


Figure 3. YonN and HBSu untwist supercoiled DNA and stimulate the activity of Nth. (A) Topoisomerase I relaxation assays of supercoiled pBSK (18 nM) in the presence of increasing concentrations of YonN (0.1, 0.2, 0.4 and 0.8 μM) or HBSu (0.0125, 0.025, 0.05, 0.1, 0.2 and 0.4 μM). Binding reactions were carried out for 20 min at 37°C in NEB buffer 4 (50 mM potassium acetate, 20 mM Tris-acetate, pH 7.9, 10 mM magnesium acetate, 1 mM DTT) before addition of topoisomerase I (0.5 units, NEB) and BSA (100 μgml^{-1}) and further incubation at 37°C for 30 min before resolving the topoisomers in a 1% (w/v) agarose gel. Lanes C1, C2 and C3 represent pBSK, pBSK plus proteinase K, and pBSK plus topoisomerase I plus proteinase K controls, respectively. (B) Time course Nth (0.5 nM) nicking assays with AP-containing pBSK (7.14 nM) in the presence of YonN (9.72 μM) or HBSu (10 μM), as indicated. Reactions were carried out in 20 mM Tris-HCl, pH 8.0, 1 mM EDTA, 1 mM DTT, 250 mM NaCl. pBSK and YonN or HBSu were incubated for 10 min at 37°C, then Nth was added for 1, 5, 15 min before the addition of Proteinase K for 30 min. Control reactions were carried out in exactly the same manner but incubated with buffer instead of YonN or HBSu. (C) The same time course Nth assay as in panel B but with DnaB (53 μM). In all cases three independent experiments were carried out and the data were quantified by densitometry. Quantification of the percentage nicking is shown in bar graphs with error bars indicating SE from triplicate experiments.

resultant Δnth *B. subtilis* strain grew marginally slower at 37°C compared to the isogenic wt *B. subtilis* strain 168 but at 30°C the two strains grew at similar rates (data not shown). Treatment with H₂O₂ (22–180 mM) revealed that Δnth was markedly more sensitive than the wt strain. Significant bacterial death was observed at >45 mM H₂O₂ (Figure 4). In comparison, the wt strain exhibited good tolerance to H₂O₂ and significant death was only apparent at concentrations >120 mM. These data confirm that Nth is an important contributor of the oxidative damage DNA repair *in vivo*.

The *dnaD-nth* operon is constitutively expressed and transiently stimulated by H₂O₂

Since the *nth* gene was shown to be important in oxidative damage repair, an important question to answer is whether the *dnaD-nth* operon is responsive to H₂O₂. In the absence of precise information about the absolute location of the promoter region (P_{*dnaD*}) of the *dnaD-nth* operon, we isolated by PCR a 600 bp fragment immediately upstream from the start codon of *dnaD* which we assumed included the entire promoter region. This fragment was cloned in the EcoRI–BamHI sites of the pDG268 plasmid immediately up-stream of (and co-directionally with) the promoterless *spoVG-lacZ* fusion gene. An entire cassette containing the 600 bp-promoter, *spoVG-lacZ* and *cat* was inserted at the *amyE* locus by a double cross-over event. The resultant P_{*dnaD*}-*lacZ catR* strain was assayed for β -galactosidase activity after H₂O₂ treatment (0.1 mM) and the data compared

to control untreated cells, as well as to the isogenic wt strain and to a control strain containing the promoterless *spoVG-lacZ* fragment at *amyE* (Figure 5A). High β -galactosidase activity was detected in the P_{*dnaD*}-*lacZ catR* strain compared to no detectable activity in the wt and promoterless *lacZ* control strains, indicating that the P_{*dnaD*} promoter was active (compare 0 mM and wt, promoterless strains in Figure 5A). Exposure to 0.1 mM H₂O₂ for 2, 5 and 7 min resulted in ~30–40% stimulation of the promoter activity compared to the control (compare the first three bars in 0.1 and 0 mM in Figure 5A), whereas at 10, 15 and 20 min the promoter activity returned to that of the control. From these data we conclude that the P_{*dnaD*} promoter is constitutively active and transiently stimulated by H₂O₂.

This was consistent with comparative RT-PCR experiments showing that the primosomal *dnaD* mRNA levels were consistently high in the presence or absence of H₂O₂ in the growth medium, compared to markedly reduced levels of the *dnaB* and *dnaI* mRNA levels after H₂O₂ exposure (Figure 5B). Treatment of cells at mid-logarithmic growth with 80 mM H₂O₂ for 30 min resulted in considerable reduction of the *dnaB*, *dnaI* mRNA levels (reduced to ~30% of the control levels) but only marginal (statistically insignificant) decrease of the *dnaD* mRNA level. These data are consistent with a constitutively active P_{*dnaD*} promoter whose activity is maintained at high levels during H₂O₂ exposure. Although the mRNA levels of *dnaB*, *dnaI* were markedly reduced in the presence of H₂O₂, it is not clear whether this is the result of

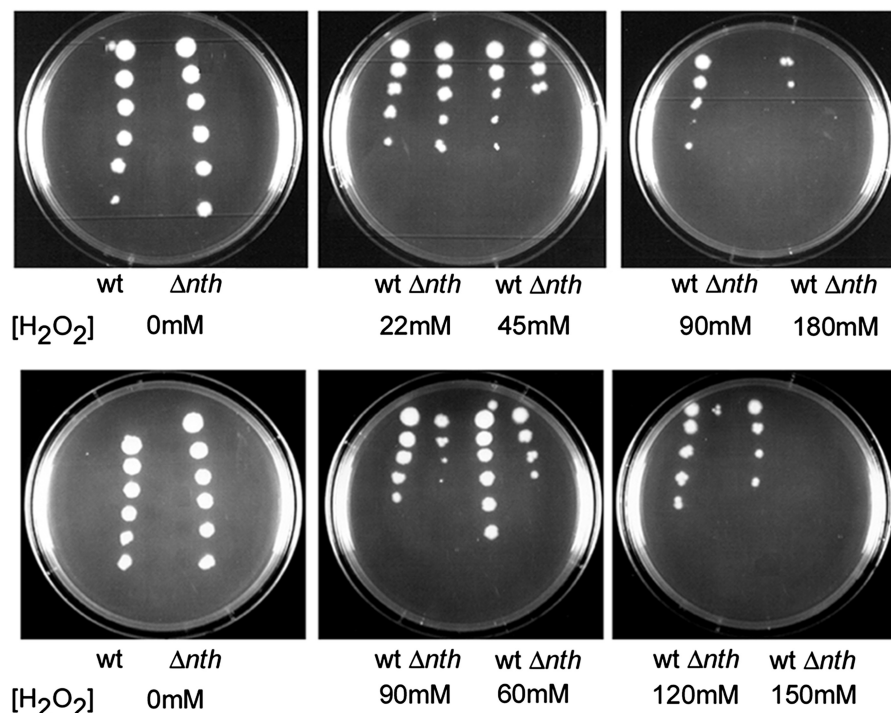


Figure 4. Deletion of *nth* increases sensitivity to H₂O₂. Samples of 1 μ l from serial dilutions (from top to bottom: undiluted, 1:10, 1:100, 1:1000, 1:10000, 1:100000) of wt *B. subtilis* 168 and Δnth control (0 mM) and H₂O₂ exposed (22, 45, 60, 90, 120, 150 and 180 mM) cultures were spotted on LA plates. Data from two independent experiments are shown in the top and bottom panels, respectively. Detailed experimental conditions are described in ‘Experimental Procedures’ section.

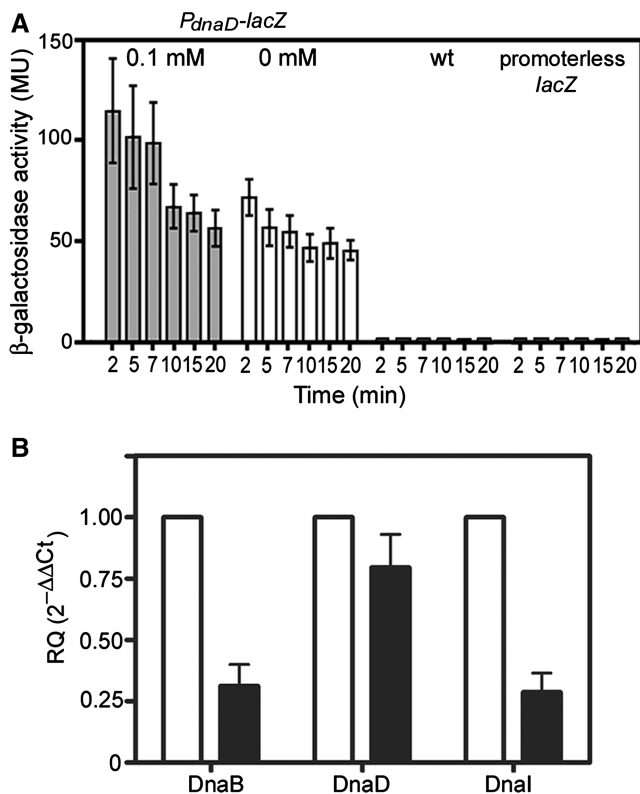


Figure 5. Constitutive expression of *dnaD* is transiently stimulated by H₂O₂ exposure. (A) The *dnaD* promoter is constitutively active. Bar charts comparing the β -galactosidase activity in the *B. subtilis* *P_{dnaD}-lacZ* strain treated with 0.1 mM H₂O₂ (shaded bars) with untreated *B. subtilis* *P_{dnaD}-lacZ* (clear bars), as indicated. Control data with the β -galactosidase activity of the isogenic wt *B. subtilis* and the promoterless *lacZ* strains are also shown. In the control wt *B. subtilis* and promoterless *lacZ* strains the β -galactosidase activity was at background levels and the bar graphs are virtually indistinguishable from the *X*-axis. The β -galactosidase activity was expressed in terms of Miller's units (MU). (B) The effect of H₂O₂ peroxide on the mRNA levels of *dnaB*, *dnaD* and *dnaI* was examined by RT-PCR. The bar graph shows relative quantification of the mRNA levels, compared to the endogenous control *r16S* (ΔC_t value), from *B. subtilis* cells after 30 min exposure to 80 mM H₂O₂ (black bars) compared to control non-exposed cells (white bars) ($\Delta\Delta C_t$ value). The bars represent the normalized means \pm standard deviation (SD) of the results from three independent experiments. The mRNA levels of *dnaB* (mean reduction = 67%, SD = 0.15, $P = 0.03$) and *dnaI* (mean reduction = 69%, SD = 0.14, $P = 0.03$) were reduced significantly but the mRNA levels of *dnaD* (mean reduction 25%, SD = 0.23, $P = 0.12$) were only marginally affected.

decreased promoter activity of the *dnaB-dnaI* operon, a consequence of increased mRNA degradation as part of the general replication stress induced by H₂O₂, or indeed a combination of the above. Further experiments, beyond the scope of this work, will be required to distinguish between these possibilities.

DISCUSSION

Bacillus subtilis is a soil bacterium exposed to a variety of oxidizing agents from external (environmental) and internal (metabolic) sources. The PerR and OhrR proteins

coordinate the oxidative stress response while the general stress response factor σ^B and the RNA polymerase-interacting thiol-based sensor Spx also contribute to the protective response via the general stress responses [(35) and references therein]. During the general stress response the expression of the stationary phase NAP Dps, controlled by σ^B , likely compacts the nucleoid to protect it against damaging agents (14), whilst during vegetative growth the PerR-controlled expression of the Dps-like protein MrgA is part of the protective oxidative stress response (35). Despite the protective roles of such NAPs lesions still arise and need to be repaired by DNA glycosylases. The substrate specificities and excision kinetics of DNA glycosylases differ significantly with the nature of the DNA substrate and with the accessibility of the targeted DNA lesions *in vivo* (14,30). With their abilities to alter the structure of the bacterial nucleoid, NAPs have the potential to participate and/or modulate DNA repair.

Here we show that the *B. subtilis* DnaD, an essential primosomal protein with NAP-like properties, HBSu (a *de facto* NAP) and YonN (a homolog of HBSu) stimulate the nicking activity of Nth in supercoiled AP-containing plasmid DNA *in vitro*. We have not been able to detect direct protein-protein interactions between the Nth and DnaD or YonN proteins despite using a range of biophysical techniques including ITC, SPR, glutaraldehyde fixing and analytical gel filtration with purified proteins. Although we cannot unequivocally eliminate weak, transient DNA-mediated physical interactions (negative data do not constitute definitive proof) or the presence of an adaptor protein that could bridge DnaD, HBSu or YonN and Nth *in vivo*, it is evident that the functional stimulation is a consequence of changes in the superhelicity of the DNA double helix mediated by the interaction of these non-specific DNA binding proteins with the DNA substrate. DnaD was previously shown to untwist supercoiled DNA by increasing the negative twist and at the same time eliminating writhe (22,26). We show here that HBSu and its YonN homolog also untwist supercoiled DNA. All three proteins were found to stimulate the Nth nicking activity. The set up of the *in vitro* nicking assay reported here gives an underestimate of the overall stimulatory effect but even relatively modest (2–3-fold) stimulation *in vivo* could have a major impact on BER on a genome-wide scale. By comparison DnaB, an essential primosomal protein with NAP-like activity but unable to untwist supercoiled DNA, did not stimulate the Nth protein. We propose that it is the DNA helix untwisting by DnaD, YonN or HBSu that indirectly stimulates the nicking activity of Nth.

The molecular mechanism of this stimulatory effect likely relates to the recognition of the estranged base by Nth. The crystal structure of the *Bacillus stearothermophilus* EndoIII (78% identical and 89% similar to the *B. subtilis* Nth) bound to a lesion-containing DNA revealed significant bending, distortion and melting of the DNA double helix at the lesion site (48). Many glycosylases exhibit some lesion specificity determined mainly by specific interactions with the lesion bases but also partly by differences in the local DNA strain and base-stacking energies. Unwinding of the DNA double helix by non-specific NAPs lowers such

energy barriers to enhance binding at the site of lesion and could potentially provide a global DNA repair regulation mechanism. NAPs coordinate the regulation of superhelicity at global and local levels which affects transcription (13) and as shown here they have the potential to regulate DNA repair too.

The *E. coli* HU, a homolog of HBSu and YonN, was shown to inhibit the rate of removal of dihydrouracil by endonuclease III when another nick was present in the opposite strand in close proximity but did not inhibit subsequent DNA synthesis and ligation during BER (49). This was suggested to be a protective mechanism to reduce the formation of double strand breaks during the repair of closely opposed lesions. HU exhibits high affinity for DNA nicks (50,51) and binds directly to them preventing access of repair nucleases and enhancing repair by DNA polymerase I and ligase. This is fundamentally different than the stimulation of the Nth nicking activity during AP repair observed here as there are no pre-formed nicks at AP sites for HU to bind and direct the Nth.

The genetic co-localization of the *dnaD* and *nth* genes in the same operon observed in *B. subtilis* is widely conserved in many gram positive Firmicutes that contain *dnaD*-like genes (Supplementary Figure S7). The list contains a range of *Bacillus*, *Lactobacillus*, *Staphylococcus*, *Acholeplasma*, *Enterococcus*, *Streptococcus* species and also *Clostridium perfringens* and *Clostridium botulinum*. Usually bacterial genes in the same operon co-operate in the same cellular functions. This is likely the case with the *dnaD*-*nth* operon too. A global transcriptome microarray analysis of *Staphylococcus aureus* in response to H₂O₂ reported transient up-regulation of the *dnaD* expression upon H₂O₂ exposure (52). Exposure to 10 mM H₂O₂ resulted in about 3× to 4× higher levels of *dnaD* mRNA after 10 min of exposure but expression returned to control levels after 20 min. This transient up-regulation of *dnaD*-*nth* operon in response to H₂O₂ exposure suggests that it is an integral part of the cellular response of *S. aureus* to H₂O₂-induced oxidative stress.

We found that the promoter of this operon in *B. subtilis* is constitutively active during exponential growth. This is consistent with the constant mRNA levels of *dnaD* throughout asynchronous growth detected before (20). Exposure to 0.1 mM H₂O₂ for 2, 5 and 7 min resulted in transient up-regulation of the promoter activity which returned to the control levels at 10, 15 and 20 min. This is somewhat analogous to the transient H₂O₂-mediated stimulation of *dnaD* expression observed in *S. aureus* by transcriptome microarray analysis (52). RT-PCR experiments revealed comparable levels of *dnaD* mRNA in H₂O₂ exposed and control cells. By comparison, the mRNA levels of the other two essential primosomal genes *dnaB* and *dnaI*, co-localized in a different distant operon, were significantly reduced upon H₂O₂ exposure. Given that the mRNA levels of *dnaB* and *dnaI* were reported to be comparable to that of *dnaD* throughout asynchronous growth (20), this down regulation may be a consequence of reduced activity of the *dnaB*-*dnaI* promoter or increased mRNA degradation or part of the replication stress response to H₂O₂ exposure or a combination of these. Down regulation of replication initiation under stress

conditions during H₂O₂ exposure, implied by the down regulation of primosomal genes, may be beneficial in order to avoid catastrophic replication fork collapse and double strand breaks at H₂O₂-induced lesions across the replicating genome. It may also allow additional time for the DNA repair mechanisms to spring into action and repair lesions before the chromosome is fit again to be replicated. Indeed AP sites form preferentially at regions undergoing DNA replication and exposure to H₂O₂ increased further their occurrence in newly replicated DNA (53).

The persistence of relatively high levels of the *dnaD* mRNA upon H₂O₂ exposure in comparison to *dnaB* and *dnaI* suggests that DnaD plays an additional role in a cellular function other than its cooperative role, with DnaB and DnaI, in the initiation of DNA replication. Normally there are only a handful of DNA replication initiation protein molecules per cell but DnaD is rather atypical as relatively large intracellular concentrations (3000–5000 molecules per cell) have been reported (54). This is suggestive that DnaD participates in other intracellular functions in addition to replication initiation. Our data show that an additional DnaD function is the stimulation of Nth during the cellular response to H₂O₂-induced oxidative damage. Its role is likely via non-specific DNA binding in the vicinity of the lesions to introduce negative twist that assists Nth binding to the lesions during BER. At the reported intracellular concentrations it is unlikely that DnaD would be able to coat the whole genome to facilitate BER. It could, however, operate at the level of distinct topological domains as suggested before (22). DnaD binding to a topological domain containing AP sites may alter its local topology by converting the plectonemic DNA into a paranemic form to facilitate BER. How DnaD targets AP sites is unknown. It may be that an unidentified adaptor protein, as suggested above, bridges Nth and DnaD and acts as a recruiter of DnaD to AP-sites. An alternative possibility is that structural deformations of the DNA double helix in the vicinity of an AP site may act as DnaD nucleation sites. Further work is required to determine the targeting mechanism.

DNA supercoiling has been proposed to act at the apex of a regulatory hierarchy that responds to environmental stress. Responsiveness of the superhelical linking number to environmental stress in collaboration with NAPs offers an attractive mechanism for the global adjustment of the gene expression profile of the cell [(55–57) and references therein]. In addition to regulation of transcription, our data suggest that this mechanism can also accommodate direct tuning of the activity of certain DNA repair enzymes such as Nth involved in BER. The genetic linkage (both genes are juxtaposed in the same operon) and functional cooperation of DnaD with Nth offers an additional H₂O₂-mediated regulatory level, above and beyond that exerted by the global superhelical density, exclusively modulating oxidative damage induced BER. The common P_{*dnaD*} promoter is transiently stimulated by H₂O₂ resulting in upregulation of DnaD and Nth that then target specifically AP sites formed by H₂O₂-induced oxidative damage.

Nth is conserved across all species including eukarya. Loss of the eukaryotic *Caenorhabditis elegans nth-1*, a homolog of the bacterial *nth* and the only BER enzyme known to initiate oxidative DNA damage repair in this organism, leads to oxidative stress and additional global gene expression changes that lead to upregulation of endogenous stress genes and downregulation of insulin-like signalling (58). The human homologs NTH1 and NTHL1 play instrumental roles in removing potentially mutagenic oxidation products of 5-methylcytosine (59). A double knock-out strain of mice (*Nth1*^{-/-}*Neil*^{-/-}) lacking both NTH1 and NEI1, the human homolog of the prokaryotic Nei endonuclease VIII (60,61), exhibited a high incidence of pulmonary and hepatic tumours in comparison to the single knock-out strains *Nth1*^{-/-} or *Neil*^{-/-} (62). Although there is no eukaryotic homolog of DnaD it will be interesting to establish whether other DNA binding proteins that alter the superhelicity of the DNA may play analogous roles in human BER by stimulating the activities of human NTH1, NTHL1 and NEI1 proteins.

SUPPLEMENTARY DATA

Supplementary Data are available at NAR Online: Supplementary Figures S1–S7. Supplementary Reference [63].

ACKNOWLEDGEMENTS

The authors thank Alan Grossman, Catherine Lee and Houra Merrikh for useful discussions, advice and help with the genetics experiments.

FUNDING

Wellcome Trust grant (091968/Z/10/Z to P.S.). C.C. was supported by a PhD studentship from the School of Chemistry, University of Nottingham. W.K.S. is supported by Veni grant 016.116.043 from the Netherlands Organisation for Scientific Research and a Gisela Thier Fellowship from the Lieden University Medical Center. Funding for open access charge: The Wellcome Trust.

Conflict of interest statement. None declared.

REFERENCES

- Dame, R.T. (2005) The role of nucleoid-associated proteins in the organization and compaction of bacterial chromatin. *Mol. Microbiol.*, **56**, 858–870.
- Thanbichler, M., Wang, S.C. and Shapiro, L. (2005) The bacterial nucleoid: a highly organized and dynamic structure. *J. Cell. Biochem.*, **96**, 506–521.
- Luijsterburg, M.S., Noom, M.C., Wuite, G.J. and Dame, R.T. (2006) The architectural role of nucleoid-associated proteins in the organization of bacterial chromatin: a molecular perspective. *J. Struct. Biol.*, **156**, 262–272.
- Maurer, S., Fritz, J. and Muskhelishvili, G. (2009) A systematic *in vitro* study of nucleoprotein complexes formed by bacterial nucleoid-associated proteins revealing novel types of DNA organization. *J. Mol. Biol.*, **387**, 1261–1276.
- Lim, J.H. and Oh, B.H. (2009) Structural and functional similarities between two bacterial chromosome compacting machineries. *Biochem. Biophys. Res. Comm.*, **386**, 415–419.
- Leonard, A.C. and Grimwade, J.E. (2005) Building a bacterial orisome: emergence of new regulatory features for replication origin unwinding. *Mol. Microbiol.*, **55**, 978–985.
- Nordström, K. and Dasgupta, S. (2001) Partitioning of the *Escherichia coli* chromosome: superhelicity and condensation. *Biochimie*, **83**, 41–48.
- Travers, A., Schneider, R. and Muskhelishvili, G. (2001) DNA supercoiling and transcription in *Escherichia coli*: The FIS connection. *Biochimie*, **83**, 213–217.
- Stoebel, D.M., Free, A. and Dorman, C.J. (2008) Anti-silencing: overcoming H-NS-mediated repression of transcription in gram-negative enteric bacteria. *Microbiology*, **154**, 2533–2545.
- Dorman, C.J. and Kane, K.A. (2009) DNA bridging and antibridging: a role for bacterial nucleoid-associated proteins in regulating the expression of laterally acquired genes. *FEMS Microbiol. Rev.*, **33**, 587–592.
- Browning, D.F., Grainger, D.C. and Busby, S.J.W. (2010) Effects of nucleoid-associated proteins on bacterial chromosome structure and gene expression. *Curr. Opin. Microbiol.*, **13**, 773–780.
- Dillon, S.C. and Dorman, C.J. (2010) Bacterial nucleoid-associated proteins, nucleoid structure and gene expression. *Nat. Rev. Microbiol.*, **8**, 185–195.
- Rimsky, S. and Travers, A. (2011) Pervasive regulation of nucleoid structure and function by nucleoid-associated proteins. *Curr. Opin. Microbiol.*, **14**, 136–141.
- Frenkiel-Krispin, D. and Minsky, A. (2006) Nucleoid organization and the maintenance of DNA integrity in *E. coli*, *B. subtilis* and *D. radiodurans*. *J. Struct. Biol.*, **156**, 311–319.
- Smits, W.K., Goranov, A.I. and Grossman, A.D. (2010) Ordered association of helicase loader proteins with the *Bacillus subtilis* origin of replication *in vivo*. *Mol. Microbiol.*, **75**, 452–461.
- Marsin, S., McGovern, S., Ehrlich, S.D., Bruand, C. and Polard, P. (2001) Early steps of *Bacillus subtilis* primosome assembly. *J. Biol. Chem.*, **276**, 45818–45825.
- Bruand, C., Ehrlich, S.D. and Janniere, L. (1995) Primosome assembly site in *Bacillus subtilis*. *EMBO J.*, **14**, 2642–2650.
- Merrikh, H., Machón, C., Grainger, W.H., Grossman, A.D. and Soutanas, P. (2011) Co-directional replication-transcription conflicts lead to replication restart. *Nature*, **470**, 554–557.
- Marston, F.Y., Grainger, W.H., Smits, W.K., Hopcroft, N.H., Green, M., Hounslow, A.M., Grossman, A.D., Craven, C.J. and Soutanas, P. (2010) When sequence comparison fails: the cryptic case of the shared domains of the bacterial replication initiation protein DnaB and DnaD. *Nucleic Acids Res.*, **38**, 6930–6942.
- Grainger, W.H., Machón, C., Scott, D.J. and Soutanas, P. (2010) DnaB proteolysis *in vivo* regulates oligomerization and its localization at *oriC* in *Bacillus subtilis*. *Nucleic Acids Res.*, **38**, 2851–2864.
- Turner, I.J., Scott, D.J., Allen, S., Roberts, C.J. and Soutanas, P. (2004) The *Bacillus subtilis* DnaD protein: a putative link between DNA remodeling and initiation of DNA replication. *FEBS Lett.*, **577**, 460–464.
- Zhang, W., Carneiro, M.J.V.M., Turner, I.J., Allen, S., Roberts, C.J. and Soutanas, P. (2005) The *Bacillus subtilis* DnaD and DnaB proteins exhibit different DNA remodelling activities. *J. Mol. Biol.*, **351**, 66–75.
- Carneiro, M.J., Zhang, W., Ioannou, C., Scott, D.J., Allen, S., Roberts, C.J. and Soutanas, P. (2006) The DNA-remodelling activity of DnaD is the sum of oligomerization and DNA-binding activities on separate domains. *Mol. Microbiol.*, **60**, 917–924.
- Zhang, W., Machón, C., Orta, A., Phillips, N., Roberts, C.J., Allen, S. and Soutanas, P. (2008) Single-molecule atomic force spectroscopy reveals that DnaD forms scaffolds and enhances duplex melting. *J. Mol. Biol.*, **377**, 706–714.
- Schneider, S., Zhang, W., Soutanas, P. and Paoli, M. (2008) Structure of the N-terminal oligomerization domain of DnaD reveals a unique tetramerization motif and provides insights into scaffold formation. *J. Mol. Biol.*, **376**, 1237–1250.
- Zhang, W., Allen, S., Roberts, C.J. and Soutanas, P. (2006) The *Bacillus subtilis* primosomal protein DnaD untwists supercoiled DNA. *J. Bacteriol.*, **188**, 5487–5493.

27. Ioannou,C., Schaeffer,P.M., Dixon,N.E. and Soutlanas,P. (2006) Helicase binding to DnaI exposes a cryptic DNA-binding site during helicase loading in *Bacillus subtilis*. *Nucleic Acids Res.*, **34**, 5247–5258.
28. Nunez-Ramirez,R., Velten,M., Rivas,G., Polard,P., Carazo,J.M. and Donate,L.E. (2007) Loading a ring: structure of the *Bacillus subtilis* DnaB protein, a co-loader of the replicative helicase. *J. Mol. Biol.*, **367**, 764–769.
29. Velten,M., McGovern,S., Marsin,S., Ehrlich,S.D., Noirot,P. and Polard,P. (2003) A two-protein strategy for the functional loading of a cellular replicative DNA helicase. *Mol. Cell*, **11**, 1009–1020.
30. Dizdaroglou,M. (2005) Base-excision repair of oxidative DNA damage by DNA glycosylases. *Mutat. Res.*, **591**, 45–59.
31. Denver,D.R., Swenson,S.L. and Lynch,M. (2003) An evolutionary analysis of the helix-hairpin-helix superfamily of DNA repair glycosylases. *Mol. Biol. Evol.*, **20**, 1603–1611.
32. Mazumder,A., Gerlt,J.A., Absalon,M.J., Stubbe,J., Cunningham,R.P., Withka,J. and Bolton,P.H. (1991) Stereochemical studies of the β -elimination reactions at aldehydic abasic sites in DNA: endonuclease III from *Escherichia coli*, sodium hydroxide, and Lys-trp-Lys. *Biochemistry*, **30**, 1119–1126.
33. Mol,C.D., Kuo,C.F., Thayer,M.M., Cunningham,R.P. and Tainer,J.A. (1995) Structure and function of the multifunctional DNA-repair enzyme exonuclease III. *Nature*, **374**, 381–386.
34. Fu,W., O'Handley,S., Cunningham,R.P. and Johnson,M.K. (1992) The role of the iron-sulfur cluster in *Escherichia coli* endonuclease III. A resonance Raman study. *J. Biol. Chem.*, **267**, 16135–16137.
35. Zuber,P. (2009) Management of oxidative stress in *Bacillus*. *Ann. Rev. Microbiol.*, **63**, 575–597.
36. Lhomme,J., Constant,J.F. and Demeunynck,M. (1999) Abasic DNA structure, reactivity, and recognition. *Biopolymers*, **52**, 65–83.
37. Lindhal,T. and Andersson,A. (1972) Rate of chain breakage at apurinic sites in double-stranded deoxyribonucleic acid. *Biochemistry*, **11**, 3618–3623.
38. Makrigiorgos,G.M., Chakrabarti,S. and Mahmood,A. (1998) Fluorescent labeling of abasic sites: a novel methodology to detect closely-spaced damage sites in DNA. *Int. J. Radiation Biol.*, **74**, 99–109.
39. Youngman,P., Poth,H., Green,B., York,K., Olmeda,G. and Smith,K. (1989) Methods for genetic manipulation, cloning, and functional analysis of sporulation genes in *Bacillus subtilis*. In Smith,I., Slepecky,R. and Setlow,P. (eds), *Regulation of Prokaryotic Development*. American Society for Microbiology, Washington, DC, pp. 65–87.
40. Antoniewski,C., Savelli,B. and Stagier,P. (1990) The *spoIIJ* gene, which regulates early developmental steps in *Bacillus subtilis*, belongs to a class of environmentally responsive genes. *J. Bacteriol.*, **172**, 86–93.
41. Xue,J. and Ahring,B.K. (2011) Enhancing isoprene production by genetic modification of the 1-deoxy-d-xylulose-5-phosphate pathway in *Bacillus subtilis*. *Applied Environ. Microbiol.*, **77**, 2399–2405.
42. Siddique,A., Buisine,N. and Chalmers,R. (2011) The transposon-like *Correia* elements encode numerous strong promoters and provide a potential new mechanism for phase variation in the meningococcus. *PLoS Genet.*, **7**, e1001277.
43. Kunst,F., Ogasawara,N., Moszer,I., Albertini,A.M., Alloni,G., Azevedo,V., Bertero,M.G., Bessieres,P., Bolotin,A., Borchert,S. et al. (1997) The complete genome sequence of the gram-positive bacterium *Bacillus subtilis*. *Nature*, **390**, 249–256.
44. Mukherjee,A., Sokunbi,A.O. and Grove,A. (2008) DNA protection by histone-like protein HU from the hyperthermophilic eubacterium *Thermotoga maritima*. *Nucleic Acids Res.*, **36**, 3956–3968.
45. Guo,F. and Adhya,S. (2007) Spiral structure of *Escherichia coli* HU $\alpha\beta$ provides foundation for DNA supercoiling. *Proc. Natl Acad. Sci. USA*, **104**, 4309–4314.
46. Swinger,K.K., Lemberg,K.M., Zhang,Y. and Rice,P.A. (2003) Flexible DNA bending in HU-DNA cocrystal structures. *EMBO J.*, **22**, 3749–3760.
47. Mouw,K.W. and Rice,P.A. (2007) Shaping the *Borrelia burgdorferi* genome: crystal structure and binding properties of the DNA-bending protein Hbb. *Mol. Microbiol.*, **63**, 1319–1330.
48. Fromme,J.S. and Verdine,G.L. (2003) Structure of a trapped endonuclease III-DNA covalent intermediate. *EMBO J.*, **22**, 3461–3471.
49. Hashimoto,M., Imhoff,B., Ali,M.M. and Kow,Y.W. (2003) HU protein of *Escherichia coli* has a role in the repair of closely opposed lesions in DNA. *J. Biol. Chem.*, **278**, 28501–28507.
50. Kamashev,D. and Rouviere-Yaniv,J. (2000) The histone-like protein HU binds specifically to DNA recombination and repair intermediates. *EMBO J.*, **19**, 6527–6535.
51. Castaing,B., Zelwer,C., Laval,J. and Boiteux,S. (1995) HU protein of *Escherichia coli* binds specifically to DNA that contains single-strand breaks or gaps. *J. Biol. Chem.*, **270**, 10291–10296.
52. Chang,W., Small,D.A., Toghrol,F. and Bentley,W.E. (2006) Global transcriptome analysis of *Staphylococcus aureus* response to hydrogen peroxide. *J. Bacteriol.*, **188**, 1648–1659.
53. Chastain,P.D. II, Nakamura,J., Rao,S., Chu,H., Ibrahim,J.G., Swenberg,J.A. and Kaufman,D.G. (2010) Abasic sites preferentially form at regions undergoing DNA replication. *FASEB J.*, **24**, 3674–3680.
54. Bruand,C., Velten,M., McGovern,S., Marsin,S., Serena,C., Ehrlich,S.D. and Polar,P. (2005) Functional interplay between the *Bacillus subtilis* DnaD and DnaB proteins essential for initiation and re-initiation of DNA replication. *Mol. Microbiol.*, **55**, 1138–1150.
55. Dorman,C.J. (2006) DNA supercoiling and bacterial gene expression. *Sci. Prog.*, **89**, 151–166.
56. Lim,H.M., Lewis,D.E., Lee,H.J., Liu,M. and Adhya,S. (2003) Effect of varying the supercoiling of DNA on transcription and its regulation. *Biochemistry*, **42**, 10718–10725.
57. Koster,D.A., Crut,A., Shuman,S., Bjornsti,M.A. and Dekker,N.H. (2010) Cellular strategies for regulating DNA supercoiling: a single-molecule perspective. *Cell*, **142**, 519–530.
58. Fensgård,Ø., Kassahun,H., Bombik,I., Rognes,T., Lindvall,J.M. and Nilsen,H. (2010) A two-tiered compensatory response to loss of DNA repair modulates aging and stress response pathways. *Aging*, **2**, 133–159.
59. David,S.S., O'Shea,V.L. and Kundu,S. (2007) Base-excision repair of oxidative DNA damage. *Nature*, **447**, 941–950.
60. Bandaru,V., Sunkara,S. and Wallace,S.S. (2002) A novel human DNA glycosylase that removes oxidative DNA damage and is homologous to *Escherichia coli* endonuclease VIII. *DNA Repair*, **1**, 517–529.
61. Hazra,T.K., Kow,Y.W., Hatahet,Z., Imhoff,B., Boldogh,I., Mokkalpati,S.K., Mitra,S. and Izumi,T. (2002) Identification and characterization of a novel human DNA glycosylases for repair of cytosine-derived lesions. *J. Biol. Chem.*, **277**, 30417–30420.
62. Chan,M.K., Ocampo-Hafalla,M.T., Vartanian,V., Jaruga,P., Kirkali,G., Koenig,K.L., Brown,S. and Lloyd,R.S. (2009) Targeted deletion of the genes encoding NTH1 and NEIL1 DNA N-glycosylases reveals the existence of novel carcinogenic oxidative damage to DNA. *DNA Repair*, **8**, 786–794.
63. Peterson,J.D., Umayan,L.A., Dickinson,T.M., Hickey,E.K. and White,O. (2001) The comprehensive microbial resource. *Nucleic Acids Res.*, **29**, 123–125.